Search for New Physics in the Two Higgs to Four b-quark Final State

by

Alice Cocoros

A dissertation submitted to The Johns Hopkins University

in conformity with the requirements for the degree of

Doctor of Philosophy

Baltimore, Maryland

June, 2017

Abstract

My thesis is about bla bla

Primary Reader: Petar Maksimovic

Secondary Reader: Morris Swartz

Acknowledgments

Thanks!

Table of Contents

List of Tables

List of Figures

Chapter 1

Introduction

Figure 1.1: Snapshot of a cloud chamber, circa 1933: the vertical line represents a positron traveling through the cloud chamber, curving due to the magnetic field applied to the chamber.

In 1869, Johann Wilhelm Hittorf discovered Cathode Rays[2], suggesting that there may be subatomic particles. By 1911, these were identified as electrons, observed in many different ways, including cloud chambers, as can be seen in Figure 1.1. Soon after, protons were discovered in 1917, followed by neutrons in 1935.

As physicists advanced the study of quantum mechanics, many new particles were discovered. These particles can be broken down into several elementary particles, whose interactions are governed by *The Standard Model* (SM).

1.1 The Standard Model

The SM describes the interaction of all elementary particles with one formula, shown in Figure 1.2. This lengthy Lagrangian can be summarized as a list of particles and mediating forces, represented in Figure 1.3.

$$-\frac{1}{2}\partial_\nu g^a_\mu \partial_\nu g^a_\mu - g_s f^{abc}\partial_\mu g^a_\nu g^b_\mu g^c_\nu - \frac{1}{4}g_s^2 f^{abc} f^{ade} g^b_\mu g^c_\nu g^d_\mu g^e_\nu +$$
$$\frac{1}{2}ig_s^2(\bar{q}^\sigma_i \gamma^\mu q^\sigma_j)g^a_\mu + \bar{G}^a\partial^2 G^a + g_s f^{abc}\partial_\mu \bar{G}^a G^b g^c_\mu - \partial_\nu W^+_\mu \partial_\nu W^-_\mu -$$
$$M^2 W^+_\mu W^-_\mu - \frac{1}{2}\partial_\nu Z^0_\mu \partial_\nu Z^0_\mu - \frac{1}{2c_w^2}M^2 Z^0_\mu Z^0_\mu - \frac{1}{2}\partial_\mu A_\nu \partial_\mu A_\nu - \frac{1}{2}\partial_\mu H \partial_\mu H -$$
$$\frac{1}{2}m_h^2 H^2 - \partial_\mu \phi^+ \partial_\mu \phi^- - M^2 \phi^+ \phi^- - \frac{1}{2}\partial_\mu \phi^0 \partial_\mu \phi^0 - \frac{1}{2c_w^2}M\phi^0\phi^0 - \beta_h[\frac{2M^2}{g^2}+$$
$$\frac{2M}{g}H + \frac{1}{2}(H^2 + \phi^0\phi^0 + 2\phi^+\phi^-)] + \frac{2M^4}{g^2}\alpha_h - igc_w[\partial_\nu Z^0_\mu(W^+_\mu W^-_\nu -$$
$$W^+_\nu W^-_\mu) - Z^0_\nu(W^+_\mu \partial_\nu W^-_\mu - W^-_\mu \partial_\nu W^+_\mu) + Z^0_\mu(W^+_\nu \partial_\nu W^-_\mu -$$
$$W^-_\nu \partial_\nu W^+_\mu)] - igs_w[\partial_\nu A_\mu(W^+_\mu W^-_\nu - W^+_\nu W^-_\mu) - A_\nu(W^+_\mu \partial_\nu W^-_\mu -$$
$$W^-_\mu \partial_\nu W^+_\mu) + A_\mu(W^+_\nu \partial_\nu W^-_\mu - W^-_\nu \partial_\nu W^+_\mu)] - \frac{1}{2}g^2 W^+_\mu W^-_\mu W^+_\nu W^-_\nu +$$
$$\frac{1}{2}g^2 W^+_\mu W^-_\nu W^+_\mu W^-_\nu + g^2 c_w^2(Z^0_\mu W^+_\mu Z^0_\nu W^-_\nu - Z^0_\mu Z^0_\mu W^+_\nu W^-_\nu) +$$
$$g^2 s_w^2(A_\mu W^+_\mu A_\nu W^-_\nu - A_\mu A_\mu W^+_\nu W^-_\nu) + g^2 s_w c_w[A_\mu Z^0_\nu(W^+_\mu W^-_\nu -$$
$$W^+_\nu W^-_\mu) - 2A_\mu Z^0_\mu W^+_\nu W^-_\nu] - g\alpha[H^3 + H\phi^0\phi^0 + 2H\phi^+\phi^-] -$$
$$\frac{1}{8}g^2\alpha_h[H^4 + (\phi^0)^4 + 4(\phi^+\phi^-)^2 + 4(\phi^0)^2\phi^+\phi^- + 4H^2\phi^+\phi^- + 2(\phi^0)^2 H^2] -$$
$$gMW^+_\mu W^-_\mu H - \frac{1}{2}g\frac{M}{c_w^2}Z^0_\mu Z^0_\mu H - \frac{1}{2}ig[W^+_\mu(\phi^0\partial_\mu\phi^- - \phi^-\partial_\mu\phi^0) -$$
$$W^-_\mu(\phi^0\partial_\mu\phi^+ - \phi^+\partial_\mu\phi^0)] + \frac{1}{2}g[W^+_\mu(H\partial_\mu\phi^- - \phi^-\partial_\mu H) - W^-_\mu(H\partial_\mu\phi^+ -$$
$$\phi^+\partial_\mu H)] + \frac{1}{2}g\frac{1}{c_w}(Z^0_\mu(H\partial_\mu\phi^0 - \phi^0\partial_\mu H) - ig\frac{s_w^2}{c_w}MZ^0_\mu(W^+_\mu\phi^- - W^-_\mu\phi^+) +$$
$$igs_w MA_\mu(W^+_\mu\phi^- - W^-_\mu\phi^+) - ig\frac{1-2c_w^2}{2c_w}Z^0_\mu(\phi^+\partial_\mu\phi^- - \phi^-\partial_\mu\phi^+) +$$
$$igs_w A_\mu(\phi^+\partial_\mu\phi^- - \phi^-\partial_\mu\phi^+) - \frac{1}{4}g^2 W^+_\mu W^-_\mu[H^2 + (\phi^0)^2 + 2\phi^+\phi^-] -$$
$$\frac{1}{4}g^2\frac{1}{c_w^2}Z^0_\mu Z^0_\mu[H^2 + (\phi^0)^2 + 2(2s_w^2 - 1)^2\phi^+\phi^-] - \frac{1}{2}g^2\frac{s_w^2}{c_w}Z^0_\mu\phi^0(W^+_\mu\phi^- +$$
$$W^-_\mu\phi^+) - \frac{1}{2}ig^2\frac{s_w^2}{c_w}Z^0_\mu H(W^+_\mu\phi^- - W^-_\mu\phi^+) + \frac{1}{2}g^2 s_w A_\mu\phi^0(W^+_\mu\phi^- +$$
$$W^-_\mu\phi^+) + \frac{1}{2}ig^2 s_w A_\mu H(W^+_\mu\phi^- - W^-_\mu\phi^+) - g^2\frac{s_w}{c_w}(2c_w^2 - 1)Z^0_\mu A_\mu\phi^+\phi^- -$$
$$g^1 s_w^2 A_\mu A_\mu\phi^+\phi^- - \bar{e}^\lambda(\gamma\partial + m_e^\lambda)e^\lambda - \bar{\nu}^\lambda\gamma\partial\nu^\lambda - \bar{u}^\lambda_j(\gamma\partial + m_u^\lambda)u^\lambda_j -$$
$$\bar{d}^\lambda_j(\gamma\partial + m_d^\lambda)d^\lambda_j + igs_w A_\mu[-(\bar{e}^\lambda\gamma^\mu e^\lambda) + \frac{2}{3}(\bar{u}^\lambda_j\gamma^\mu u^\lambda_j) - \frac{1}{3}(\bar{d}^\lambda_j\gamma^\mu d^\lambda_j)] +$$
$$\frac{ig}{4c_w}Z^0_\mu[(\bar{\nu}^\lambda\gamma^\mu(1+\gamma^5)\nu^\lambda) + (\bar{e}^\lambda\gamma^\mu(4s_w^2 - 1 - \gamma^5)e^\lambda) + (\bar{u}^\lambda_j\gamma^\mu(\frac{4}{3}s_w^2 -$$
$$1 - \gamma^5)u^\lambda_j) + (\bar{d}^\lambda_j\gamma^\mu(1 - \frac{8}{3}s_w^2 - \gamma^5)d^\lambda_j)] + \frac{ig}{2\sqrt{2}}W^+_\mu[(\bar{\nu}^\lambda\gamma^\mu(1+\gamma^5)e^\lambda) +$$
$$(\bar{u}^\lambda_j\gamma^\mu(1+\gamma^5)C_{\lambda\kappa}d^\kappa_j)] + \frac{ig}{2\sqrt{2}}W^-_\mu[(\bar{e}^\lambda\gamma^\mu(1+\gamma^5)\nu^\lambda) + (\bar{d}^\lambda_j C^\dagger_{\lambda\kappa}\gamma^\mu(1+$$
$$\gamma^5)u^\lambda_j)] + \frac{ig}{2\sqrt{2}}\frac{m_e^\lambda}{M}[-\phi^+(\bar{\nu}^\lambda(1-\gamma^5)e^\lambda) + \phi^-(\bar{e}^\lambda(1+\gamma^5)\nu^\lambda)] -$$
$$\frac{g}{2}\frac{m_e^\lambda}{M}[H(\bar{e}^\lambda e^\lambda) + i\phi^0(\bar{e}^\lambda\gamma^5 e^\lambda)] + \frac{ig}{2M\sqrt{2}}\phi^+[-m_d^\kappa(\bar{u}^\lambda_j C_{\lambda\kappa}(1-\gamma^5)d^\kappa_j) +$$
$$m_u^\lambda(\bar{u}^\lambda_j C_{\lambda\kappa}(1+\gamma^5)d^\kappa_j] + \frac{ig}{2M\sqrt{2}}\phi^-[m_d^\lambda(\bar{d}^\lambda_j C^\dagger_{\lambda\kappa}(1+\gamma^5)u^\kappa_j) - m_u^\kappa(\bar{d}^\lambda_j C^\dagger_{\lambda\kappa}(1-$$
$$\gamma^5)u^\kappa_j] - \frac{g}{2}\frac{m_u^\lambda}{M}H(\bar{u}^\lambda_j u^\lambda_j) - \frac{g}{2}\frac{m_d^\lambda}{M}H(\bar{d}^\lambda_j d^\lambda_j) + \frac{ig}{2}\frac{m_u^\lambda}{M}\phi^0(\bar{u}^\lambda_j\gamma^5 u^\lambda_j) -$$
$$\frac{ig}{2}\frac{m_d^\lambda}{M}\phi^0(\bar{d}^\lambda_j\gamma^5 d^\lambda_j) + \bar{X}^+(\partial^2 - M^2)X^+ + \bar{X}^-(\partial^2 - M^2)X^- + \bar{X}^0(\partial^2 -$$
$$\frac{M^2}{c_w^2})X^0 + \bar{Y}\partial^2 Y + igc_w W^+_\mu(\partial_\mu\bar{X}^0 X^- - \partial_\mu\bar{X}^+ X^0) + igs_w W^+_\mu(\partial_\mu\bar{Y}X^- -$$
$$\partial_\mu\bar{X}^+ Y) + igc_w W^-_\mu(\partial_\mu\bar{X}^- X^0 - \partial_\mu\bar{X}^0 X^+) + igs_w W^-_\mu(\partial_\mu\bar{X}^- Y -$$
$$\partial_\mu\bar{Y}X^+) + igc_w Z^0_\mu(\partial_\mu\bar{X}^+ X^+ - \partial_\mu\bar{X}^- X^-) + igs_w A_\mu(\partial_\mu\bar{X}^+ X^+ -$$
$$\partial_\mu\bar{X}^- X^-) - \frac{1}{2}gM[\bar{X}^+ X^+ H + \bar{X}^- X^- H + \frac{1}{c_w^2}\bar{X}^0 X^0 H] +$$
$$\frac{1-2c_w^2}{2c_w}igM[\bar{X}^+ X^0\phi^+ - \bar{X}^- X^0\phi^-] + \frac{1}{2c_w}igM[\bar{X}^0 X^-\phi^+ - \bar{X}^0 X^+\phi^-] +$$
$$igMs_w[\bar{X}^0 X^-\phi^+ - \bar{X}^0 X^+\phi^-] + \frac{1}{2}igM[\bar{X}^+ X^+\phi^0 - \bar{X}^- X^-\phi^0]$$

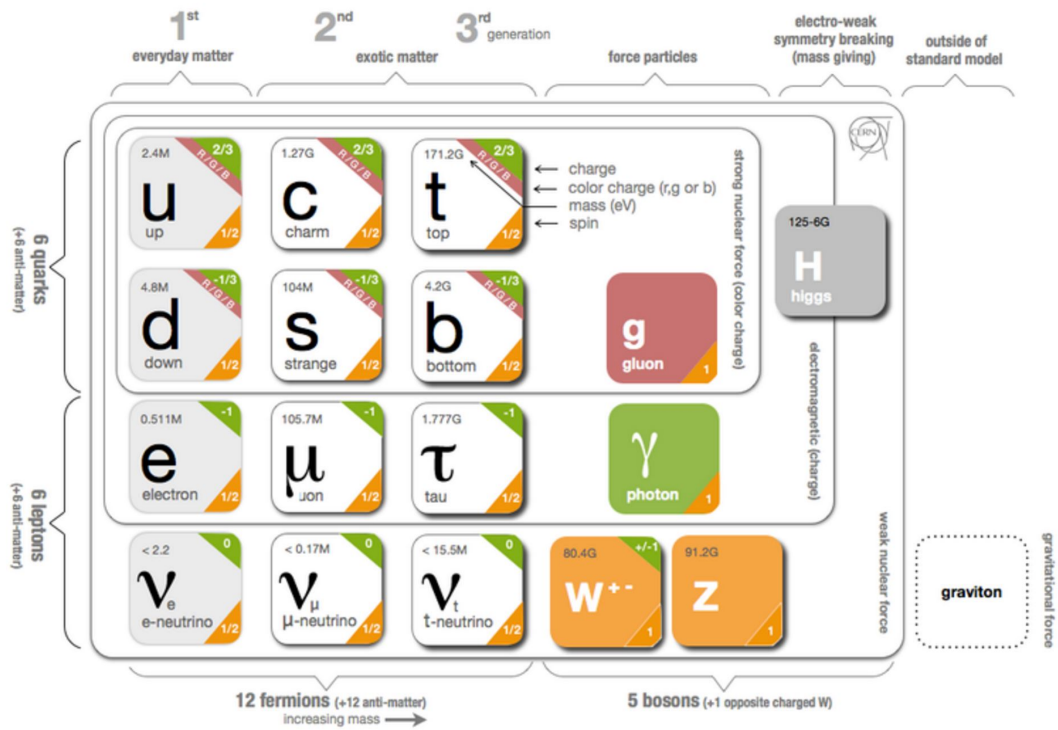Figure 1.2: The Standard Model Lagrangian.

Figure 1.3: Table of Standard Model particles. Image from CERN[1].

1.1.1 Leptons

The electron is one of the most well known elementary particles. There exist two heavier "versions" of the electron: the muon (μ) which is $\sim$ 200 times as massive as the electron, and the tau (τ) which is $\sim$ 4000 times as massive as the electron. Each of these particles is negatively charged, where the charge is equivalent to -1 which corresponds to - 1.602×10^{-19} Coulombs.

For each of these particles, there exists a corresponding neutrino, so we have ν_e, ν_μ and ν_τ. The neutrinos as defined by the SM are chargeless and massless, although experiments have proved that at least two out of three neutrinos observed in nature have mass.

A corresponding anti-particle exists for each of these six particles: $\bar{e}$ (e^+), $\bar{\mu}$ (μ^+,), $\bar{\tau}$ (τ^+), $\bar{\nu}_e$, $\bar{\nu}_\mu$, and $\bar{\nu}_\tau$. Note that, while neutrinos are chargeless, the anti-particle for the electron, muon, and tau, all have positive (or opposite of their corresponding particle) charge.

In addition to charge and mass, particles also have spin, or the intrinsic angular momentum of a particle. All of the above mentioned particles, known as leptons, have spin $\frac{1}{2}$ (or $-\frac{1}{2}$), which means they are fermions. The spin of a particle allows us to define helicity, also known as handedness. This is the sign of the projectino of the particle's spin vector onto its momentum vector. A particle is said to be right-handed if the spin and momentum align, and left-handed if the spin and momentum point opposite each other. In the Standard Model, there can be difference between left-handed and right-handed particles. For example, we have observed that all neutrinos are left-handed, while all anti-neutrinos are right-handed, which is currently still inexplicable.

1.1.2 Quarks

Many of the particles discovered in the twentieth century are composite particles called hadrons, made up of quarks. There are six quarks: t*up (u)*,*down (d)*, *strange (s)*, *charm (c)*, *bottom (b)*, and *top (t)*.

The u, c and t quarks have charge $+\frac{2}{3}$ and the d, s and b quarks have charge $-\frac{1}{3}$. Quarks also have each a different mass. For every quark there is an anti-quark: $\overline{u}, \overline{d}, \overline{s}, \overline{c}, \overline{b}$ and $\overline{t}$. Quarks are also fermions, and therefore have a spin of $\frac{1}{2}$ or $-\frac{1}{2}$.

In addition to charge (by which we mean electric charge), mass, and spin, quarks also have a second kind of charge, known as color. While electric charge allows particles to interact through the electromagnetic force, color charge allows particles to interact through a different type of force, called the strong force. Quarks can be red, green, or blue colored, and anti-quarks can be anti-red, anti-green, or anti-blue colored. In nature, we only see color neutral particles, which is why quarks are only observed as combinations forming composite particles. These composite particles made up of quarks are color neutral because they either contain one quark of each color, or a quark of a particular color and a quark of the corresponding anti-color. For example, the proton is made up of on u and two d quarks, so one of these must be red, one must be green, and one must be blue.

1.1.3   Representation of Interactions

The Standard Model describes how matter particles, described above, interact with each other through the exchange of force mediating particles. Let us consider a simple scenario of electron electron interaction, which happens through the exchange of the electromagnetic mediating particle known as the photon. This process can be drawn using a vertex, as can be seen in Figure 1.4. This

$$\gamma$$

$$e^- \qquad\qquad e^-$$
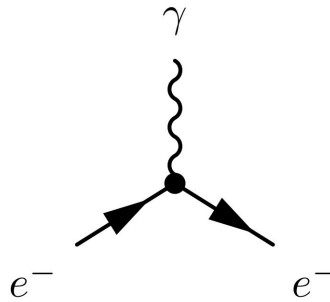
Figure 1.4: Visual representation of the interaction between two electrons (straight lines) and a photon (wiggly line).

vertex can be arranged and combined with other vertices in a variety of ways to represent different interactions between electrons, positrons, and photons. For example, we can consider the case where two electrons are propelled towards each other. Using two of the vertex pictured in 1.4, we can see that this must result in two electrons, as can be seen in Figure 1.5, where time propagates to the right on the x-axis, and distance is represented on the y-axis. Alternatively, if we were to consider the interaction between an electron an a positron, which can be represented as an electron with an arrow pointing backwards in time, we can see that the resulting process is described by Figure Fig:Intro:Feynman2, where an electron and a positron annihilate to a photon, which produces an-electron positron pair. In both of these diagrams, we notice that charge is
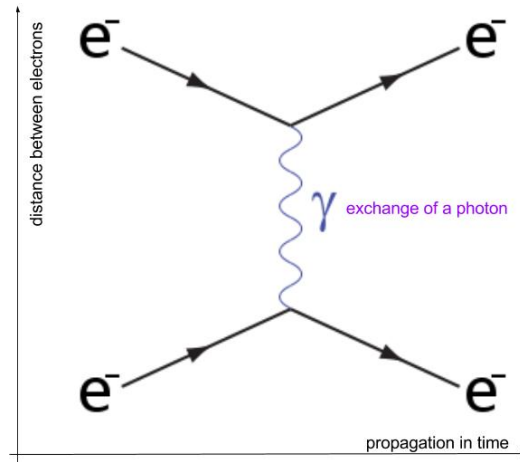
Figure 1.5: A Feynman Diagram showing the interaction of two electrons. Time increases to the right on the x-axis, and the y-axis represents the distance between the two electrons.

conserved on either side of the diagram. Many more diagrams can be made with this vertex, combining it with other vertices that involve a photon as well. In understanding these diagrams, we can explain three of the four fundamental forces at a qualitative level, below, while also introducing new theories in later chapters that have motivated the search for new particles.

1.1.4 The Electromagnetic Force:

Quantum electrodynamics (QED) describes how the electromagnetic force behaves at the quantum level. The force carrier of QED is the photon, γ, which is massless and moves at the speed of light. This theory can be described fully by Figure 1.4, since the photon has neutral electric charge and cannot couple to itself. Many experiments have performed precision measurements of QED properties, verifying that they match SM predictions extremely well.
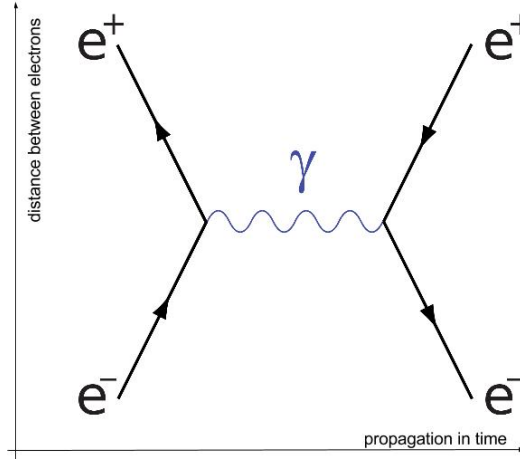
Figure 1.6: A Feynman Diagram showing the annihilation of a positron and an electron.

1.1.5 The Strong Force:

Quantum Chromodynamics (QCD) describes quantum interactions related to the strong force. The force carrier of QCD is the gluon, g, which is massless and moves at the speed of light. The gluon does have color charge, just as the quarks do, and therefore there are a number of vertices in QCD, as shown in Figure 1.7. As mentioned before, each quark has a color charge, and each anti-quark has an anti-color charge. Since color must be conserved, we can see that the gluon must carry a color and an anti-color for the vertices in Figure 1.7 to be true. Naively, since there are three colors, one would think there are nine gluons, or nine possible combination of three colors and three anticolors. These are summarized below:

$$\frac{r\bar{r}+b\bar{b}+g\bar{g}}{\sqrt{3}}$$

$$\frac{r\bar{b}+b\bar{r}}{\sqrt{2}} \qquad \frac{r\bar{g}+g\bar{r}}{\sqrt{2}} \qquad \frac{b\bar{g}+g\bar{b}}{\sqrt{2}} \qquad \frac{r\bar{r}-b\bar{b}}{\sqrt{2}}$$

$$\frac{-i(r\bar{b}-b\bar{r})}{\sqrt{2}} \qquad \frac{-i(r\bar{g}-g\bar{r})}{\sqrt{2}} \qquad \frac{-i(b\bar{g}-g\bar{b})}{\sqrt{2}} \qquad \frac{r\bar{r}+b\bar{b}-2g\bar{g}}{\sqrt{6}}$$

9
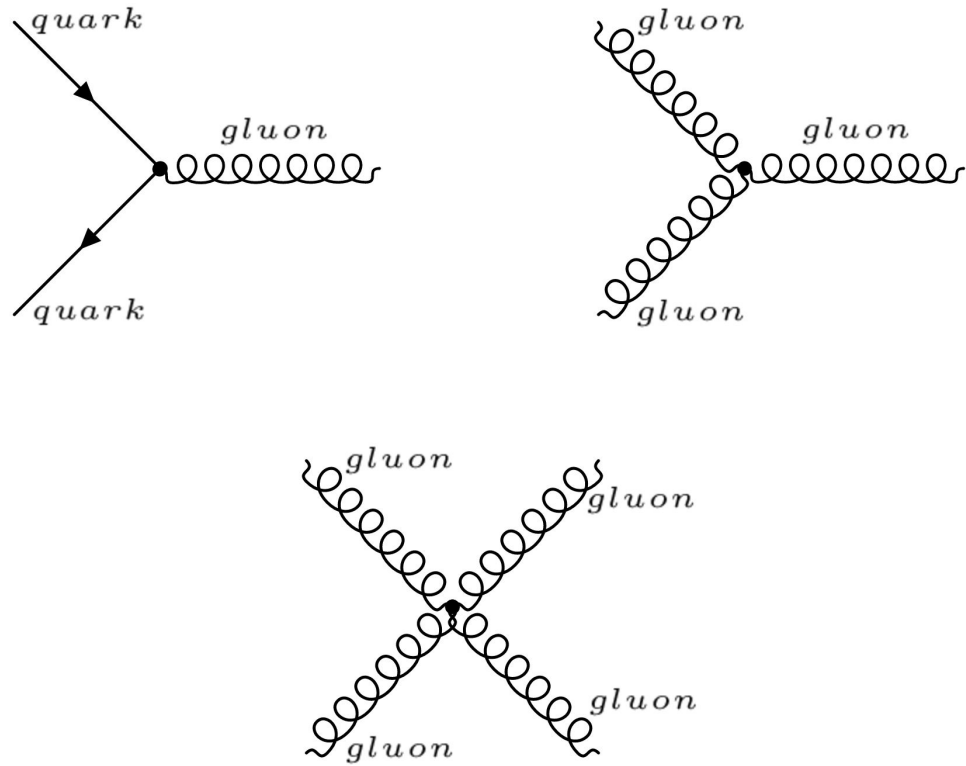
Figure 1.7: QCD interactions can be described by three vertices. The curly line represents gluons, while the straight lines represent quarks. Since gluons are colored, they can interact with themselves.

Particles comprised of quarks must be color neutral, both mesons (two-quark bound states) and baryons (three-quark bound states). We know that a particle can be neutral if it contains either quarks with color anti-color, or all three color quarks. Then since the combination of red, green, and blue is neutral, the first combination listed would be color neutral. However, color neutral particles must be non-interacting, otherwise colorless baryons would emit these gluons and interact with one another through the strong force, which we do not observe in nature. Therefore, this first combination is not possible, and there are only eight gluons, called the color octet.

The strong force is responsible for hadronization, or the production of many quarks and gluons when quarks are smashed apart due to an event such as a proton-proton collision. As quarks drift apart after the collision, a color tube of self-interacting gluons is created between the quarks. These tubes are stretched as the quarks drift further apart, increasing energy in the tube due to the constant force exerted from stretching. At distances of roughly 10^{-15} m, it becomes more energetically favorable for two new quarks to be created from the vacuum, through the process shown in the top left vertex in Figure 1.7. If these new quarks are still too energetic to be contained in a particle, this process will repeat until the energy has been sufficiently decreased for all new quark pairs to stay bound. This property is known as confinement, and is critical to the understanding of hadronic activity within a particle detector.

1.1.6 The Weak Force:

When the universe had first begun and was still very hot, the weak force and the electromagnetic force were combined to form the electroweak force. At this time, the electroweak interaction was mediated by four massless bosons: W_1, W_2, W_3 and B. As the universe cooled, the bosons eventually began interacting with the Higgs field (addressed in the following section), and soon, the bosons that interacted with fermions were no longer these four, but a superposition of them. We can write this superpositions as

$$\begin{pmatrix} \gamma \\ Z \end{pmatrix} = \begin{pmatrix} \cos\theta_W & \sin\theta_W \\ -\sin\theta_W & \cos\theta_W \end{pmatrix} \begin{pmatrix} B \\ W_3 \end{pmatrix} \tag{1.1}$$

$$W^{\pm} = \frac{(W_1 \mp iW_2)}{\sqrt{2}} \tag{1.2}$$

11

where θ_W, the mixing angle, is a parameter of the SM. Therefore, while γ is the force carrier for the electromagnetic force, the Z, W^+, and W^- are the force carriers for the weak force. The weak interaction is interesting because it only acts on left-handed particles and right-handed anti-particles.

The vertexes describing the weak force interactions can be found in Figure 1.8. While the photon is massless, the three weak force carriers are not. The Z
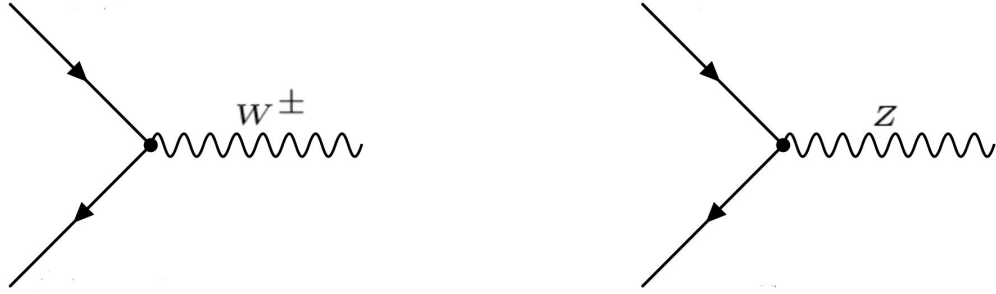
Figure 1.8: Weak interactions can be described by the following vertices. The wavy lines represent bosons, while the straight lines represent any particle where the appropriate quantities are conserved.

Boson has a mass of 91.2 GeV/c^2 (where protons have a mass of ~ 1 GeV/c^2 for reference). The Z boson allows particles to interact with their anti-particles through the weak force. For example, the process $Z \to e^- e^+$ is permitted, but the process $Z \to \mu^+ e^-$ is not permitted. The Z boson can couple to both electrically charged and neutral particles, as well as particles with and without color.

The $W^\pm$ boson, which has a mass of 80.4 GeV/c^2, also couples pairs of fermions. Rather than linking particles and anti-particles like the Z boson, it allows the flavors within a generation to interact. For example, a W^+ boson

can decay to two quarks ($W^+ \rightarrow u\bar{d}$), and a W^- can decay to a lepton and its neutrino ($W^- \rightarrow \mu\nu_\mu$). Since the $W^\pm$ is electrically charged, electric charge must be conserved at each vertex, and also $\gamma \rightarrow W^+W^-$ is allowed. The decay $Z \rightarrow W^+W^-$ is also a potential vertex.

The probability of a W decaying to different generations is dictated by the CKM Matrix, where each of these values has been experimentally measured:

$$\begin{pmatrix} V_{ud} & V_{us} & V_{ub} \\ V_{cd} & V_{cs} & V_{cb} \\ V_{td} & V_{ts} & V_{tb} \end{pmatrix} = \begin{pmatrix} 0.974 & 0.225 & 0.004 \\ 0.225 & 0.973 & 0.041 \\ 0.009 & 0.040 & 0.999 \end{pmatrix} \qquad (1.3)$$

where $|V_{ij}|^2$ is the probability that a quark i decays to a quark j through the emission of a W.

Since all other particles decay through a W to a lighter particle, this explains why our world is built with up quarks, down quarks, and electrons (the building blocks of atoms).

1.1.7   Mass and the Higgs Boson

The Higgs Boson is the most recent confirmed Standard Model particle. It is related to the mass of other SM particles. To understand how this is so, we will look at the Higgs potential, which we can write as $\sim (\phi^2 - \eta^2)^2$ for the purpose of explanation. This is plotted in Figure 1.9. The potential is symmetric about the y-axis, or the axis with units of energy. In the early universe while everything was still very hot, the energies of particles were so high that the bumps at the bottom of the potential had no consequence. As the universe cooled, however, these minima became important, and one must be chosen. This is known as spontaneous symmetry breaking.
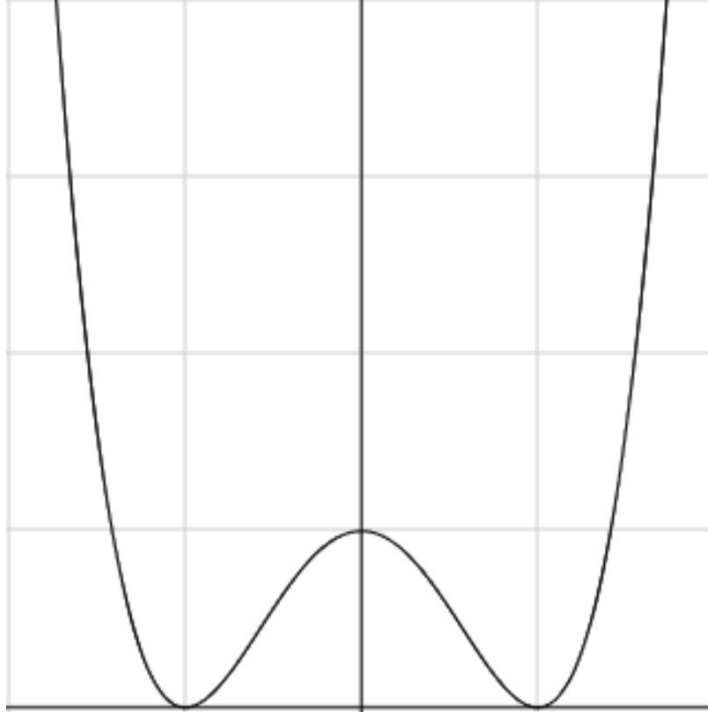
Figure 1.9: Approximation of the Higgs potential. While the shape is symmetric about the y-axis, the function is not symmetric about the minima.

Once the universe had cooled sufficiently, the Higgs field took on a vacuum expectation value (VEV), or an average value in empty space, which was non-zero. This VEV couples to electroweak interactions, as referenced in the previous section, and the photon and weak force bosons mixed to form the states we know today. The spontaneously broken Higgs field also couples to quarks, electrons, muons, taus, Z bosons, and $W^{\pm}$ bosons. However, it does not couple to neutrinos, so the explanation for their mass must lie elsewhere.

While we have been referring to the Higgs field, the Higgs boson is the particle that was recently discovered at the LHC in 2012. This particle is an excitation of the Higgs field in the same way that a photon is an excitation of the electromagnetic field. The SM Higgs has no charge, no spin, and a mass of

126 GeV. It couples to anything with mass (aside from the neutrinos), so it can also couple to itself. These vertexes take the form shown in Figure 1.10.
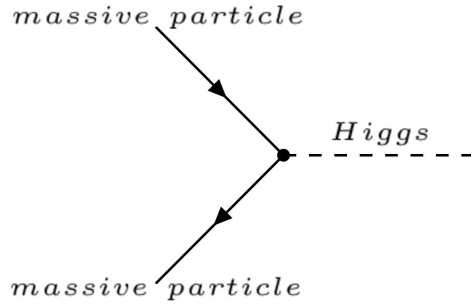
Figure 1.10: The Higgs Vertex. The dashed line is the Higgs Boson and the straight lines are any massive particle.

1.2 Rounding Up the Standard Model Particles

In total, including particles of different colors and all anti-particles, there exist 61 particles in the SM. We can describe their interactions easily using the vertices presented in each section So to recap, there are, once we count all the colors and anti-particles, 61 particles in the standard model. We know they interact, and we can pictorally express a number of complex interactions using the Feynman diagram. For example, consider the diagrams in Figure 1.11. These are important physics processes by which two gluons interact with quarks to produce two Higgs, which is central to the topic of this thesis. This shows an example of the different kind of processes possible using Feynman diagrams: two protons collide and gluons inside of them interact with different quarks to produce two Higgs bosons (left) or one Higgs boson that then produces two

Figure 1.11: Left: Two gluons interact with a quark, while each gluon interacts with an additional different quark, and these additional different quarks interact with a shared fourth quark and each pair of quarks interacts to form a Higgs boson. Right: Two gluons interact with a quark, while each gluon interacts with an additiona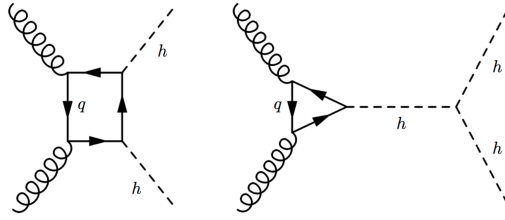l quark, and these additional different quarks interact with each other to form a Higgs boson, which interacts with two Higgs bosons. The result of both of these processes is a final state with two Higgs.

Higgs bosons (right).

While this description has been qualitative, and has not drawn distinction between what has been experimentally determined and what has been predicted in the SM, the SM is quite self-consistent. There are only 19 parameters which are experimentally determined, most of which are masses.

1.3 Beyond the Standard Model

While the SM is an impressive feat of mathematics and experiments, it leaves many questions unanswered. For example, the SM only accounts for baryonic matter, which is estimated to be 4.6% of the universe. A remaining 24% is accounted for by dark matter, which can only be gravitationally detected, while the rest of the universe is said to be made up of dark energy.

The SM is also missing one of the four fundamental forces, gravity. While we have convincing understanding of quantum mechanics and general relativity, a unification for these two theories has yet to be discovered. Neutrino mass is

unaccounted for by the SM. The Higgs mass is much lower than one might expect from the SM. The universe is dominated by matter, rather than anti-matter.

Many questions remain that require answers beyond the SM, and so we search for new particles at the LHC in hopes of providing new insight into these difficult problems.

Chapter 2

Introduction

2.1   Theoretical overview

The discovery of a boson with a mass of approximately 125GeV, and with properties close to those expected for the Higgs boson (H) of the SM [3, 4], has stimulated interest in the exploration of the Higgs potential, described in 1. The production of a pair of Higgs bosons within the SM is a rare process that is sensitive to the structure of this potential through the self-coupling mechanism of the Higgs boson, as discussed in the previous chapter. An effective way to look for new physics is to examine the production cross section of two H at the LHC.

A cross section tells us the probability of a particular final state of events. This depends on the initial conditions of the collision, ie the energy going into the collision and what you are colliding. The unit used for cross section is barn, with $1b = 100 \text{fm}^2 = 10^{-28} \text{m}^2$. In the SM, the cross section for the production of two H bosons in pp collisions at 8 TeV is 10.0 ± 1.4 fb for the gluon-gluon fusion process [5, 6], which lies beyond the reach of analyses based on the first run of the CERN LHC. An increase in the cross section beyond SM expectation would

be a smoking gun for new physics. This can happen in one of two ways: there are new particles which decay to HH that contribute to the production of HH, or there are new processes, or additional vertices, that contribute to the production of HH. The first is called "resonant" production, since the increase in cross section is from a resonance (new particle), and the second is called "non-resonant", since it is a new Feynman diagram but not a new particle causing an increase in the cross section.

2.2   Resonant Production

Many theories beyond the SM (BSM) suggest different ways in which the cross section for the production of two Hwould increase, based onthe existence of heavy particles that can couple to a pair of Higgs bosons. Models with a warped extra dimension (WED), as proposed by Randall and Sundrum [7], postulate the existence of one spatial extra dimension compactified between two fixed points, commonly called branes. The region between the branes is referred to as bulk, and controlled through an exponential metric. The gap between the two fundamental scales of nature, such as the Planck scale (M_{Pl}), and the electroweak scale, is controlled by a warp factor (k) in the metric, which corresponds to one of the fundamental parameters of the theory. The brane where the density of the extra dimensional metric is localized is called the "Planck brane", while the other, where the Higgs field is localized, is called the "TeV brane". It is common in the literature to define the reduced Planck mass, $\overline{M_{Pl}} \equiv M_{Pl}/\sqrt{8\pi}$. This class of models predicts the existence of new particles, such as the spin-0 radion [8, 9, 10], and the spin-2 first Kaluza–Klein

(KK) excitation of the graviton [11, 12, 13].

There are two possible ways of describing a KK graviton from the standpoint of WED that depend on the choice of localization for the SM matter fields. In the RS1 model, only gravity is allowed to propagate in the extra-dimensional bulk, and with the KK-graviton couplings to matter fields fully defined by $k/\overline{M_{Pl}}$ [7]. For the possibility of particles in the bulk (the so-called bulk RS model), the coupling of the KK graviton to matter depends on the choice for the localization of the SM bulk fields. This paper uses the scenario of Ref. [14] as the starting point, where the propagation of SM fields is allowed in the bulk, and follows the characteristics of the SM gauge group, with the right-handed top quark localized on the TeV brane (so called elementary top hypothesis).

The radion is an additional element of WED models that is needed to stabilize the size of the extra dimension l. It is usual to express the benchmark points of the model in terms of the dimensionless quantity $k/\overline{M_{Pl}}$, and the mass scale $\Lambda_{\mathrm{R}} = \sqrt{6}e^{-kl} \times \overline{M_{Pl}}$, with the latter interpreted as the ultraviolet cutoff of the theory [15]. The addition of a scalar-curvature term can induce a mixing between the scalars radion and Higgs boson [15, 16], this possibility can be grounded on microscopic theories (see for example [17]). Due to electroweak precision tests this mixing is expected to be small, for an updated reference see for example [18]. In the interpretations of the constraints derived in this note we neglect the possibility of Higgs-radion mixing.

For the KK-graviton resonance, the choice of the localization of the SM matter fields potentially modifies the kinematics of the signal and drastically modifies the production and decay [19]. The physics of the radion from other side has little dependence on the choice of scenario [15] and therefore we do not

need to specify between RS1 and bulk RS. Supersymmetric models also predict one spin-0 resonance that, when sufficiently massive, decays to a pair of SM Higgs bosons. Those would be additional Higgs bosons [20, 21]. The signal modeling for a spin-0 particle is identical if it is a radion or an additional Higgs boson.

The tools used to calculate the cross sections for the production of KK graviton in the bulk and RS1 models are described in Ref. [22, 23]. The implementation of the calculations is described in Ref. [24]. In analogy with the Hboson, the radion field is predominantly produced through gluon-gluon fusion [25, 26]. The cross section for radion production is calculated at NLO electroweak and next-to-next-to-leading logarithmic QCD accuracy, using the recipe suggested in Ref. [15]. This recipe consists of multiplying the radion cross section based on the fundamental parameter of the theory, Λ_{R}, by a K-factor calculated for SM-like Hboson production through gluon-gluon fusion [27, 28]. The calculations are performed for the SM-like Hboson with masses up to 1TeV. They are considered constant above 1TeV. We use the CTEQ6L PDF [29] in these calculations. No mixing between a radion and the Hboson is considered in this paper. The absolute value for the production cross section scales with $(k/\overline{M_{Pl}})^2$ for the KK Graviton [19] and with $1/\Lambda_{\mathrm{R}}^2$ for the radion [30].

We compare the experimental results to the radion production cross section for $\Lambda_{\mathrm{R}} = 1$ and $3TeV$. In the first case, the WED theory predicts a cross section that can be detected at LHC [31], but is challenged by the constraints derived from the electroweak precision measurements [32]. This specific model is excluded up to $M_{\mathrm{X}} = 1.1TeV$ by the previous $X \to HH$ searches [33, 31]. In contrast, the predicted cross section for $\Lambda_{\mathrm{R}} = 3TeV$ is a factor of 9 times smaller,

but the theory is less constrained by these searches. We consider exclusively the $gg \to X$ production, with $\mathcal{B}(\text{radion} \to HH) \approx 25\%$ in the mass range under consideration.

Searches for narrow particles decaying to two Higgs bosons have already been performed by the ATLAS [34, 33, 35] and CMS [36, 31, 37] collaborations in ppcollisions at $\sqrt{s} = 7$ and 8 TeV. Until now their reach was limited to $M_X = 1.5 TeV$. Moreover, some of the models that predict the coupling of the new resonance to HH also expect it to couple to W$^+$W$^-$ or Z^{0}Z^0 [38]. Searches for these final states were performed by ATLAS and CMS [39, 40, 41, 42, 43].

Bibliography

[1] CERN, "GO ON A PARTICLE QUEST AT THE FIRST CERN WEBFEST," https://cds.cern.ch/journal/CERNBulletin/2012/35/News%20Articles/1473657, 2012.

[2] "Preliminary communications on electric discharges in rarefied gases," Monatsberichte der Kÿniglich Preussischen Akademie der Wissenschaften zu Berlin, p. 286, 1876.

[3] S. Chatrchyan *et al.*, "Observation of a new boson at a mass of 125 GeV with the CMS experiment at the LHC," *Phys. Lett. B*, vol. 716, p. 30, 2012.

[4] G. Aad *et al.*, "Observation of a new particle in the search for the Standard Model Higgs boson with the ATLAS detector at the LHC," *Phys. Lett. B*, vol. 716, p. 1, 2012.

[5] D. de Florian and J. Mazzitelli, "Higgs Boson Pair Production at Next-to-Next-to-Leading Order in QCD," *Phys. Rev. Lett.*, vol. 111, p. 201801, 2013.

[6] J. Baglio, A. Djouadi, R. GrÃűber, M. M. MÃijhlleitner, J. Quevillon, and M. Spira, "The measurement of the Higgs self-coupling at the LHC: theoretical status," *JHEP*, vol. 04, p. 151, 2013.

[7] L. Randall and R. Sundrum, "A large mass hierarchy from a small extra dimension," *Phys. Rev. Lett.*, vol. 83, p. 3370, 1999.

[8] W. D. Goldberger and M. B. Wise, "Modulus stabilization with bulk fields," *Phys. Rev. Lett.*, vol. 83, p. 4922, 1999.

[9] O. DeWolfe, D. Z. Freedman, S. S. Gubser, and A. Karch, "Modeling the fifth dimension with scalars and gravity," *Phys. Rev. D*, vol. 62, p. 046008, 2000.

[10] C. Csaki, M. Graesser, L. Randall, and J. Terning, "Cosmology of brane models with radion stabilization," *Phys. Rev. D*, vol. 62, p. 045015, 2000.

[11] H. Davoudiasl, J. L. Hewett, and T. G. Rizzo, "Phenomenology of the Randall-Sundrum Gauge Hierarchy Model," *Phys. Rev. Lett.*, vol. 84, p. 2080, 2000.

[12] C. Csaki, M. L. Graesser, and G. D. Kribs, "Radion dynamics and electroweak physics," *Phys. Rev. D*, vol. 63, p. 065002, 2001.

[13] K. Agashe, H. Davoudiasl, G. Perez, and A. Soni, "Warped Gravitons at the LHC and Beyond," *Phys. Rev. D*, vol. 76, p. 036006, 2007.

[14] A. L. Fitzpatrick, J. Kaplan, L. Randall, and L.-T. Wang, "Searching for the Kaluza-Klein Graviton in Bulk RS Models," *JHEP*, vol. 09, p. 013, 2007.

[15] G. F. Giudice, R. Rattazzi, and J. D. Wells, "Graviscalars from higher dimensional metrics and curvature Higgs mixing," *Nucl. Phys. B*, vol. 595, p. 250, 2001.

[16] D. Dominici, B. Grzadkowski, J. F. Gunion, and M. Toharia, "The Scalar sector of the Randall-Sundrum model," *Nucl. Phys. B*, vol. 671, p. 243, 2003.

[17] I. Antoniadis and R. Sturani, "Higgs graviscalar mixing in type I string theory," *Nucl. Phys. B*, vol. 631, p. 66, 2002.

[18] N. Desai, U. Maitra, and B. Mukhopadhyaya, "An updated analysis of radion-higgs mixing in the light of LHC data," *JHEP*, vol. 10, p. 093, 2013.

[19] A. Oliveira and R. Rosenfeld, "Hidden sector effects on double higgs production near threshold at the LHC," *Phys. Lett. B*, vol. 702, p. 201, 2011.

[20] A. Djouadi, "The anatomy of electroweak symmetry breaking. Tome II: the Higgs bosons in the minimal supersymmetric model," *Phys. Rept.*, vol. 459, p. 1, 2008.

[21] R. Barbieri, D. Buttazzo, K. Kannike, F. Sala, and A. Tesi, "One or more Higgs bosons?" *Phys. Rev. D*, vol. 88, p. 055011, 2013.

[22] K. Agashe, O. Antipin *et al.*, "Warped Extra Dimensional Benchmarks for Snowmass 2013," in *Community Summer Study 2013: Snowmass on the Mississippi (CSS2013) Minneapolis, MN, USA, July 29-August 6, 2013*, 2013. [Online]. Available: http://cp3-origins.dk/research/units/ed-tools

[23] P. de Aquino, K. Hagiwara, Q. Li, and F. Maltoni, "Simulating graviton production at hadron colliders," *JHEP*, vol. 06, p. 132, 2011. [Online]. Available: http://feynrules.irmp.ucl.ac.be/wiki/RSmodel

[24] A. Oliveira, "Gravity particles from Warped Extra Dimensions, a review. Part I - KK Graviton," 2014, submitted on arXiv.

[25] U. Mahanta and A. Datta, "Search prospects of light stabilized radions at Tevatron and LHC," *Phys. Lett. B*, vol. 483, p. 196, 2000.

[26] H. Davoudiasl, J. L. Hewett, and T. G. Rizzo, "Experimental probes of localized gravity: On and off the wall," *Phys. Rev. D*, vol. 63, p. 075004, 2001.

[27] S. Catani, D. de Florian, M. Grazzini, and P. Nason, "Soft gluon resummation for Higgs boson production at hadron colliders," *JHEP*, vol. 07, p. 028, 2003.

[28] S. Heinemeyer *et al.*, "Handbook of LHC Higgs Cross Sections: 3. Higgs Properties," 2013, submitted on arXiv.

[29] P. M. Nadolsky, H.-L. Lai, Q.-H. Cao, J. Huston, J. Pumplin, D. Stump, W.-K. Tung, and C.-P. Yuan, "Implications of CTEQ global analysis for collider observables," *Phys. Rev. D*, vol. 78, p. 013004, 2008.

[30] V. Barger and M. Ishida, "Randall-Sundrum Reality at the LHC," *Phys. Lett. B*, vol. 709, p. 185, 2012.

[31] V. Khachatryan *et al.*, "Search for resonant pair production of Higgs bosons decaying to two bottom quark-antiquark pairs in proton-proton collisions at 8 TeV," *Phys. Lett. B*, vol. 749, p. 560, 2015.

[32] P. Archer, M. Carena, A. Carmona, and M. Neubert, "Higgs Production and Decay in Models of a Warped Extra Dimension with a Bulk Higgs," *JHEP*, vol. 01, p. 060, 2015.

[33] G. Aad *et al.*, "Search for Higgs boson pair production in the $b\bar{b}b\bar{b}$ final state from pp collisions at $\sqrt{s} = 8$ TeV with the ATLAS detector," *Eur. Phys. J. C*, vol. 75, p. 412, 2015.

[34] ——, "Search For Higgs Boson Pair Production in the $\gamma\gamma b\bar{b}$ Final State using *pp* Collision Data at $\sqrt{s} = 8$ TeV from the ATLAS Detector," *Phys. Rev. Lett.*, vol. 114, p. 081802, 2015.

[35] ——, "Searches for Higgs boson pair production in the $hh \to bb\tau\tau, \gamma\gamma WW^*, \gamma\gamma bb, bbbb$ channels with the ATLAS detector," *Phys. Rev. D*, vol. 92, p. 092004, 2015.

[36] V. Khachatryan *et al.*, "Searches for heavy Higgs bosons in two-Higgs-doublet models and for $t \to ch$ decay using multilepton and diphoton final states in *pp* collisions at 8 TeV," *Phys. Rev. D*, vol. 90, p. 112013, 2014.

[37] ——, "Searches for a heavy scalar boson H decaying to a pair of 125 GeV Higgs bosons hh or for a heavy pseudoscalar boson A decaying to Zh, in the final states with $h \to \tau\tau$," *Phys. Lett. B*, vol. 755, pp. 217–244, 2016.

[38] J. Brehmer *et al.*, "The Diboson Excess: Experimental Situation and Classification of Explanations; A Les Houches Pre-Proceeding," 2015, submitted on arXiv.

[39] G. Aad *et al.*, "Search for high-mass diboson resonances with boson-tagged jets in proton-proton collisions at $\sqrt{s} = 8$ TeV with the ATLAS detector," *JHEP*, vol. 12, p. 055, 2015.

[40] ——, "Search for production of WW/WZ resonances decaying to a lepton, neutrino and jets in pp collisions at $\sqrt{s} = 8$ TeV with the ATLAS detector," *Eur. Phys. J. C*, vol. 75, p. 209, 2015, [Erratum: 10.1140/epjc/s10052-015-3593-4].

[41] ——, "Search for resonant diboson production in the $\ell\ell q\bar{q}$ final state in pp collisions at $\sqrt{s} = 8$ TeV with the ATLAS detector," *Eur. Phys. J. C*, vol. 75, p. 69, 2015.

[42] V. Khachatryan *et al.*, "Search for massive resonances in dijet systems containing jets tagged as W or Z boson decays in pp collisions at $\sqrt{s} = 8$ TeV," *JHEP*, vol. 08, p. 173, 2014.

[43] ——, "Search for massive resonances decaying into pairs of boosted bosons in semi-leptonic final states at $\sqrt{s} = 8$ TeV," *JHEP*, vol. 08, p. 174, 2014.

[44] ATLAS and CMS Collaborations, "Combined Measurement of the Higgs Boson Mass in pp Collisions at $\sqrt{s} = 7$ and 8 TeV with the ATLAS and CMS Experiments," *Phys. Rev. Lett.*, vol. 114, p. 191803, 2015.